CHALMERS
UNIVERSITY OF TECHNOLOGY

Calibration in RIS-Aided Integrated Sensing, Localization and Communication Systems

Citation for the original published paper (version of record):
Ghazalian, R., Zheng, P., Chen, H. et al (2025). Calibration in RIS-Aided Integrated Sensing, Localization and Communication Systems. IEEE Wireless Communications, In Press: 1-8.
http://dx.doi.org/10.1109/MWC.2025.3600619

Calibration in RIS-aided Integrated Sensing, Localization and Communication Systems

Reza Ghazalian, Pinjun Zheng, Hui Chen, Cuneyd Ozturk, Musa Furkan Keskin, Vincenzo Sciancalepore, Sinan Gezici, Tareq Y. Al-Naffouri, and Henk Wymeersch

***Abstract*—Reconfigurable intelligent surfaces (RISs) are key enablers for integrated sensing and communication (ISAC) systems in the sixth-generation (6G) communication era. With the capability of dynamically shaping the channel, RISs can enhance communication coverage. Additionally, RISs can serve as additional anchors with high angular resolution to improve localization and sensing services in extreme scenarios. However, knowledge of anchors' states such as position, orientation, and hardware impairments are crucial for localization and sensing applications, requiring dedicated calibration, including geometry and hardware calibration. This paper provides an overview of various types of RIS calibration, their impacts, and the challenges they pose in ISAC systems.**

***Index Terms*—Localization, sensing, calibration, RIS, 6G.**

I. Introduction

In the sixth-generation (6G) mobile communication system, the integration of sensing and communication into a single system will enable high-accuracy and high-resolution sensing capabilities, benefiting both functions. Being part of the sensing functionality, the localization service focuses on accurately estimating the locations of connected users while the broader sensing capability also encompasses the detection and estimation of passive objects. Reconfigurable intelligent surfaces (RISs) play a crucial role in integrated sensing and communication (ISAC) systems by shaping and optimizing the wireless channel for both communication and sensing purposes [1]. RISs are typically constructed as planar surfaces comprising a large number of controllable elements that can alter the incident electromagnetic (EM) wave's characteristics, such as phase, amplitude, frequency, or even polarization [2]. Several types of RISs have been introduced in literature, including passive RIS (PRIS), hybrid RIS (HRIS), active RIS (ARIS), simultaneous transmission and reflection (STAR) RIS, and beyond diagonal RIS (BD-RIS) [3]. Each of these types has its own advantages and disadvantages when applied in localization, sensing, and communication systems. These factors may include performance, signal control overhead, and complexity of signal processing algorithms. Implementation of sensing, localization and communication functions requires knowledge of RISs' geometry and hardware states (e.g., position, orientation, RIS phase configuration, and RIS steering vectors). Consequently, calibration in all these aspects is one of the most crucial and challenging tasks in practice [4], [5], yet it is often neglected in theoretical studies on RIS.

Calibration can be roughly categorized into two types, namely, geometry and hardware. In *geometry calibration*, the position and orientation of the RIS are estimated, which is essential for RIS-aided sensing or localization systems, where RISs serve as reference points. For RIS-aided communication systems, knowledge of the RIS location can facilitate location-based optimization of the RIS phase profile. In *hardware calibration*, the states of the RIS hardware (e.g., mutual coupling, pixel failure, and non-linearity of the power amplifier) is estimated and compensated for, to prevent performance degradation. Figure 1 presents an overview of these primary types of RIS calibration. Despite the importance of calibration in RIS-aided ISAC systems, research in this field has largely overlooked calibration problems. To address this gap, in this paper, we highlight the negative impact of inaccurate calibration on both localization and communication performance, examine the effect of the RIS topology on the calibration, and describe the main calibration methodologies. We also present case studies of joint calibration and user equipment (UE) localization and of the trade-offs between communication and sensing performance in ISAC under hardware impairments. These case studies focus on passive RIS, as these currently represent the most practically viable and commercially available solution. Finally, we discuss future research directions in this area.

II. Why do we need RIS calibration?

In this section, we elaborate on two main model mismatches due to non-calibrated RIS and then quantify their impact on localization and communication.

A. Model Mismatches

1) Geometric Mismatches: Accurate knowledge of an RIS's position and orientation is crucial for localization and sensing and beneficial for communication. However, real-world deployment introduces uncertainties due to poor calibration, environmental changes, and RIS mobility (e.g., RIS-equipped vehicles). These inaccuracies lead to model mismatches where the network assumes an incorrect RIS location and orientation, causing errors in localization references and beam misalignment. Effective calibration mitigates these issues, reducing overhead and improving system reliability.

This paper is partially supported by the SNS JU project 6G-DISAC under the EU's Horizon Europe research and innovation Program under Grant Agreement No. 101139130 as well as the Swedish Research Council (VR) under project No. 2022-03007 and project No. 2024-04390, the King Abdullah University of Science and Technology (KAUST) Office of Sponsored Research (OSR) under Award ORA-CRG2021-4695, the European Union under the Italian National Recovery and Resilience Plan (NRRP) of NextGenerationEU, partnership on "Telecommunications of the Future" (PE00000001 - program "RESTART"), and the EU Horizon project TIMES (Grant No. 101096307).

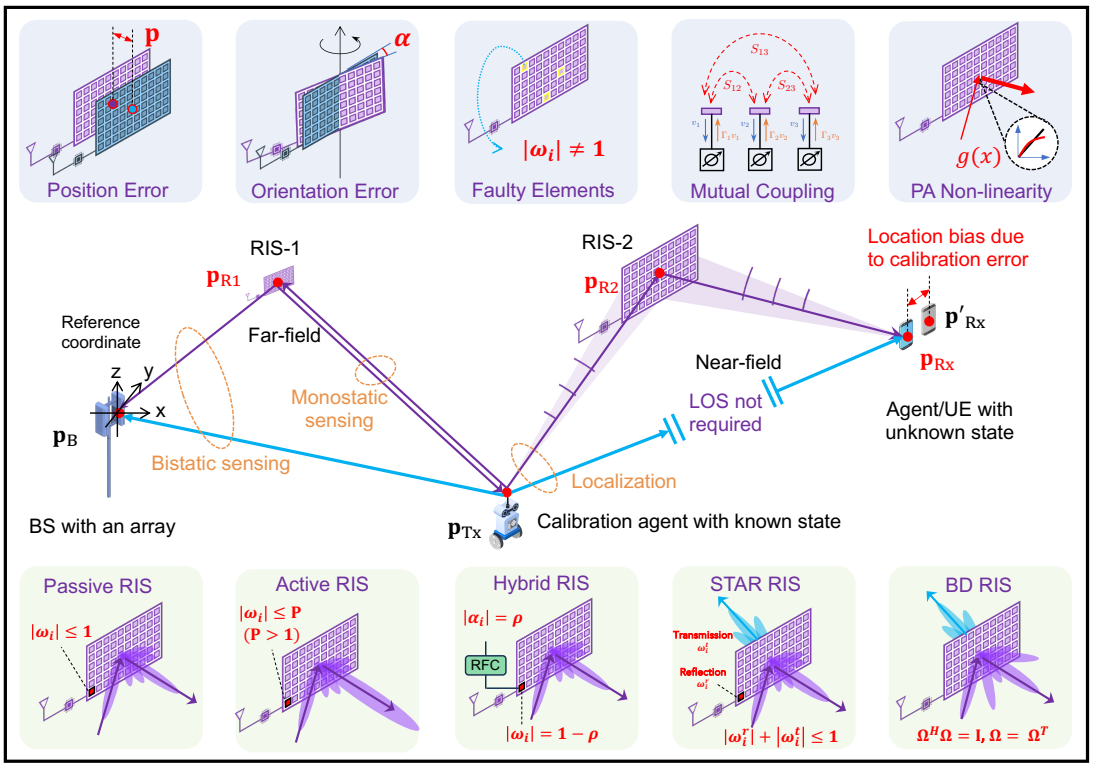

Fig. 1. Illustration of RIS calibration approaches and various RIS architectures in ISAC systems. The **top row** illustrates representative imperfections, including geometric mismatches in RIS position and orientation as well as hardware impairments such as faulty elements, mutual coupling, and power amplifier (PA) non-linearity, which lead to model mismatches and can degrade localization and communication performance. The **middle row** shows RIS in ISAC scenarios, where known anchors enable sensing of an RIS agent, and UEs with unknown states support joint localization and calibration. The **bottom row** presents different RIS architectures, including passive, active, hybrid, and STAR-RIS. To fully unlock the potential of RIS-aided systems, both agent-based calibration (e.g., RIS-1, where transmitter (Tx) and receiver (Rx) positions are known) and joint localization and calibration (e.g., RIS-2, involving UEs with unknown states) can be applied in far-field and near-field conditions.

2) Hardware Mismatches: RIS, as a low-cost technology is also susceptible to various hardware-related effects, which typical signal processing methods are unaware of.

- *Pixel Failure:* Individual RIS elements may fail due to internal defects (e.g., manufacturing errors, bit flips) or external factors (e.g., dust, rain, ice) [6]. While pre-deployment calibration can address manufacturing issues, failures can occur unpredictably in operation, necessitating dynamic detection.
- *Mutual Coupling:* In dense RIS arrays, elements interact electromagnetically, distorting the radiation pattern. Unlike conventional antennas, RIS elements are excited passively, complicating calibration. This issue becomes severe in ultra-dense arrays like holographic MIMO/RIS [7].
- *Phase-Dependent Amplitude Variations*: Real-world RIS elements exhibit amplitude variations based on phase shifts, deviating from idealized unity-gain models [8]. Accurate modeling of these effects is essential for localization and communication performance.
- *Other Hardware Impairments*: Additional distortions arise in different RIS architectures, including power amplifier non-linearity in active RISs, phase noise in hybrid RISs, and inaccuracies in reflection coefficients, due to inaccuracies in load impedance. Each RIS system requires tailored calibration to mitigate these effects.

3) Other Mismatches: In addition to geometric and hardware mismatches, other inherent mismatches, such as beam squint (e.g., frequency-dependent beam angles) or near-field (NF) effects (e.g., wavefront curvature), arise from the impact of more complicated hardware and channels than those assumed during algorithm development. These mismatches do not require calibration, but should be tackled by relying on estimators operation on accurate models, which is beyond this article's scope.

B. Impact of Model Mismatches on Localization

Geometric and hardware mismatches in RIS calibration degrade localization performance. To understand the impact of such model mismatches, the theory of mismatched estimation provides a useful tool [9]. Penalties due to such mismatched operation can be predicted analytically via the misspecified Cramér-Rao bound (MCRB), a generalization of the classical Cramér-Rao bound (CRB), accounting for model mismatches. In the following, we provide some examples to show the impact of geometry mismatch and hardware impairments through the MCRB analysis.

1) Localization Performance under Geometry Mismatch: Figure 2 shows the MCRB on the position estimation (also known as the position error bound (PEB)) for different levels of geometry errors and RIS sizes, evaluated in both far-field (FF) and NF scenarios. In both scenarios, the localization error in the mismatch-free case reduces with increased transmit

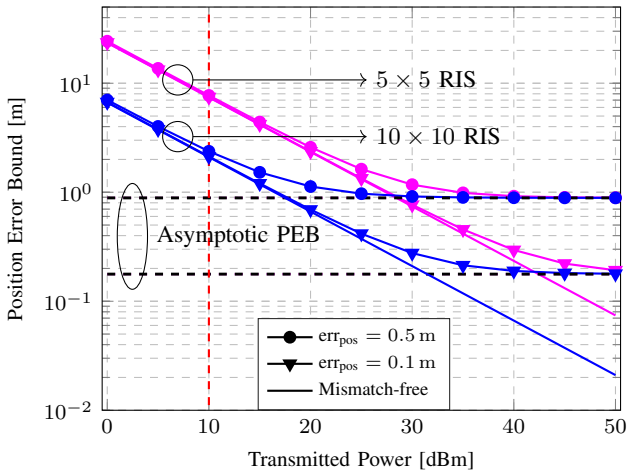

(a) FF Evaluation Using Planar-Wave Model

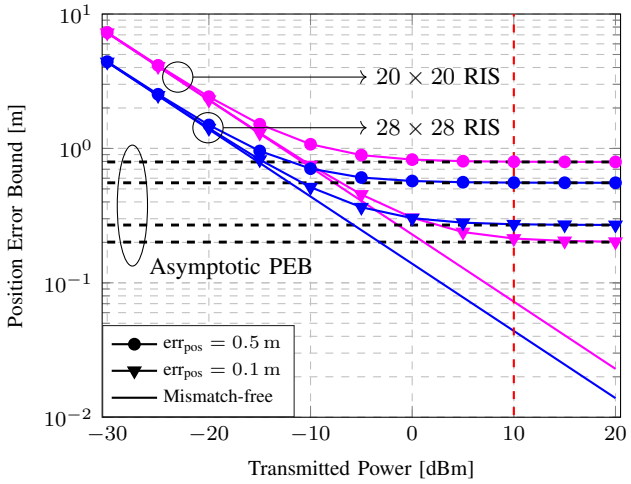

(b) NF Evaluation Using Spherical-Wave Model

Fig. 2. PEB versus transmit power is evaluated under varying RIS geometry errors in an RIS-aided downlink localization system. The setup includes a single-antenna access point at $[-5, 5, 10]^{\mathsf{T}}$m, a single-antenna UE at $[0, 3, 1]^{\mathsf{T}}$m, and a RIS at $[0, 0, 3]^{\mathsf{T}}$m, oriented along the positive y-axis. We consider 16 pilots at 28 GHz with 400 MHz bandwidth and 128 subcarriers. The power spectral density (PSD) of noise is $-173.855\,\text{dBm/Hz}$, with a noise figure of 10 dB. PEBs follow the MCRB with RIS position error modeled as $\tilde{\mathbf{p}} = \bar{\mathbf{p}} + \mathbf{u}$, where $\mathbf{u} = \text{err}_{\text{pos}} \times [1, 1, 1]^{\mathsf{T}}$. We assess both (a) FF and (b) NF scenarios, using planar and spherical wave models, respectively. A 20×20 RIS yields a Rayleigh distance of 3.87 m, exceeding the RIS–UE distance (3.61 m), indicating operation in the NF regime. Note that the x-axis ranges differ between the two subfigures. A red dashed vertical line marks the 10 dBm tick in both plots to aid visual alignment.

power. However, in the presence of RIS geometry errors, both thermal noise and model mismatch contribute to localization errors. Specifically, the position error bound aligns with the mismatch-free case at low transmit power levels, indicating that localization performance is primarily noise-limited. Conversely, at high transmit power levels, localization performance becomes mismatch-dominated and eventually saturates at a certain performance limit (asymptotic PEB). Generally, a more severe geometry mismatch results in a higher asymptotic PEB. Therefore, the PEB can always be analyzed in the noise-dominant (low transmit power) and mismatch-dominant (high transmit power) regions.

We can observe that in the FF scenario shown in Fig. 2(a), increasing the RIS size significantly improves performance in the noise-dominant region, but has no impact in the mismatch-dominant region. This is because a larger RIS size boosts the received power, thereby improving the signal-to-noise ratio (SNR), which is the bottleneck in the noise-dominant region. However, in mismatch-dominant regions, where SNR is sufficiently high, increasing the RIS size provides no additional benefit. Here, geometry mismatch—represented by the bias term derived from minimizing the Kullback-Leibler (KL) divergence—remains independent of RIS size in the FF scenario. Nonetheless, too large an RIS size can significantly influence geometric relationships due to NF effects in channel modeling. As shown in Fig. 2(b), when NF effects are considered, a larger RIS can significantly reduce the mismatch-free bound and the PEB in noise-dominant regions compared to the FF scenario. This is because, in addition to enhanced received power, a larger RIS in the NF introduces more geometric information through the spherical-wave model. Meanwhile, the mismatch-dominant region is also influenced by RIS size, as the asymptotic PEBs for different RIS sizes under the same RIS position error no longer coincide. This suggests that NF geometric relationships are dependent on RIS size. However, the impact of RIS size on the asymptotic PEB does not exhibit a clear trend. Due to the complexity of the spherical-wave model, the same level of mismatch does not necessarily produce a greater effect for larger RISs. Additionally, we observe that the localization error can be significantly higher than the calibration error. For example, as demonstrated in Fig. 2(a), a $0.5\,\text{m}$ calibration error in RIS position can result in a localization error of approximately $0.9\,\text{m}$. Apart from that, small RIS orientation errors also lead to large positioning errors when users are far away from the RIS.

2) Localization Performance under Hardware Impairments: Next, we examine the impact of pixel failures and mutual coupling on localization. Figure 3(a) shows, for the scenario in Fig. 1 with RIS-2 under line of sight (LoS) blockage between Tx and Rx, that *pixel failures*, where RIS elements fail independently with probability p_{fail}, degrade localization accuracy. At low SNR, performance aligns with the failure-free case, but at high SNR, errors saturate at a limit dictated by model mismatches, leading to up to two orders of magnitude loss when $p_{\text{fail}} = 2\%$. Additionally, Rician fading in the RIS-Rx link (captured by the K-factor) further reduces accuracy, as the stochastic non-line of sight (NLoS) components do not provide location information. Hence, even a small fraction of faulty pixels can significantly impair localization at high SNR. Similarly, *mutual coupling* distorts the RIS radiation pattern and increases power consumption. As shown in [7], denser RIS elements or larger RIS sizes intensify these effects, severely degrading channel estimation, a key step for both localization and communication.

C. Impact of Model Mismatches on Communication

In this section, we will demonstrate that communication is generally less affected by model mismatches than localization or sensing. Since this is obvious for geometry mismatches,

our focus will be on hardware impairments. We have selected pixel failure and mutual coupling, for which we present a quantitative analysis. We analyze each factor individually without comparing mismatches, as their physical origins and impacts differ.

1) Trade-off Between Communication and Localization under Pixel Failures: To assess the impact of pixel failures on localization and communication, we consider a transmission scheme split into pilot transmissions for localization and data transmissions for communication. In an NF scenario with LoS blockage, as shown for RIS-2 in Fig. 1, RIS profiles during the pilot phase illuminate potential UE locations within a known uncertainty region. The highest-power beam identified during the pilot phase is reused during data transmission. Figure 3(b) shows the trade-off between localization accuracy (lower bound (LB) from MCRB analysis [9]) and spectral efficiency across different pixel failure probabilities p_{fail}, by sweeping the relative pilot and data power. Spectral efficiency remains largely stable with respect to p_{fail}, while localization accuracy deteriorates noticeably. This discrepancy arises because communication depends on the end-to-end composite channel, whereas localization relies on geometric information inferred from RIS phase shifts. Thus, pixel failures mainly degrade localization unless they significantly impact SNR.

2) Impact of Inter-element Distance on Communication and Localization: Figure 4 illustrates the performance of a joint localization and communication system aided by a PRIS with mutual coupling. In this RIS-aided communication setup, the asymptotic PEB (localization metric, the horizontal lines in Fig. 2) and spectral efficiency (communication metric) are evaluated across various inter-element distances of the RIS. Figure 4 reveals that a reduction in the inter-element distance of the RIS causes stronger mutual coupling, which in turn degrades both localization and communication performance. However, after precise calibration, these performance losses due to mutual coupling can be effectively mitigated, for both localization and communication. Additionally, it is observed that localization is more sensitive to RIS mutual coupling compared to communication. These observations emphasize the necessity of accurate calibration.

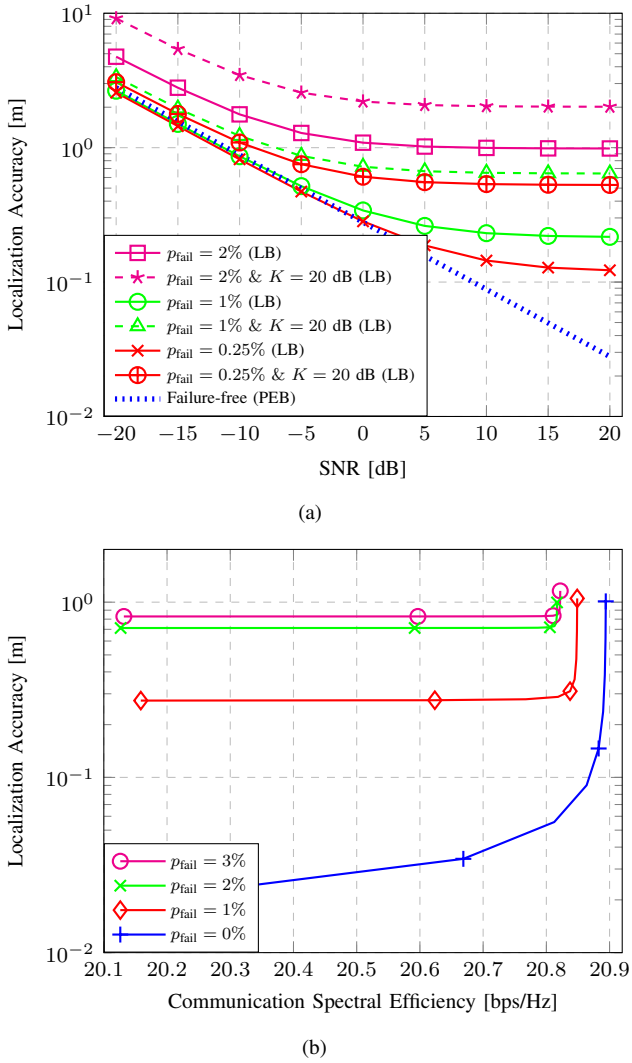

Fig. 3. (a) Theoretical limits on localization root mean square error (RMSE) vs. SNR under pixel failures and Rician fading, and (b) trade-offs between localization RMSE and communication spectral efficiency under pixel failures, using the setup from [10]. An 20×20 RIS is considered. The base station is located at $15 \times [-1\,1\,1]^{\mathsf{T}}/\|[-1\,1\,1]\|$ in (a) and at $10\times[-1\,1\,1]^{\mathsf{T}}/\|[-1\,1\,1]\|$ in (b). The user is located at $3\times[1\,1\,1]^{\mathsf{T}}/\|[1\,1\,1]\|$ in (a) and at $4 \times [1\,1\,1]^{\mathsf{T}}/\|[1\,1\,1]\|$ in (b). The considered p_{fail} values are selected based on the commonly employed range of values in the literature (e.g., [6]).

D. Effect of RIS Architectures

RIS architectures affect calibration in RIS-aided ISAC systems, with all types impacted by geometry mismatches. Orientation errors notably degrade angle-of-arrival (AOA) and angle-of-departure (AOD) measurements, while time-of-arrival (TOA) methods primarily suffer from SNR degradation and waveform distortions. Hardware mismatches differ among RIS types, but pixel failures and reflection coefficient impairments are common. These faults mostly reduce SNR in non-coherent methods but severely affect coherent processing.

PRISs depend on TOA and AOA/AOD for calibration, whereas *HRIS* simplify calibration by adding local sensing capabilities [11]. *ARISs* improve localization and communication via signal amplification but add thermal noise and exacerbate the impact of mutual coupling, which can hurt performance if unmanaged. Calibration is complicated by phase-dependent amplitude changes, requiring an optimal amplification balance [12]. *BD-RIS*, with inter-connected multiport designs, offers flexibility but increases calibration complexity due to extra parameters and possible hardware failures. Finally, *STAR-RIS* poses additional challenges; two-layer designs suffer from mutual coupling between transmission and reflection layers, while single-layer versions face phase control impairments, needing frequent calibration. Thus, STAR-RIS requires more sophisticated calibration than passive, active, or hybrid RIS.

III. Calibration Methodologies

In this section, we describe two main calibration types for the ISAC system. Although categorized into geometry and hardware, calibration errors often occur simultaneously with varying severity, necessitating prioritization of critical aspects and diverse calibration algorithms for optimal performance. To

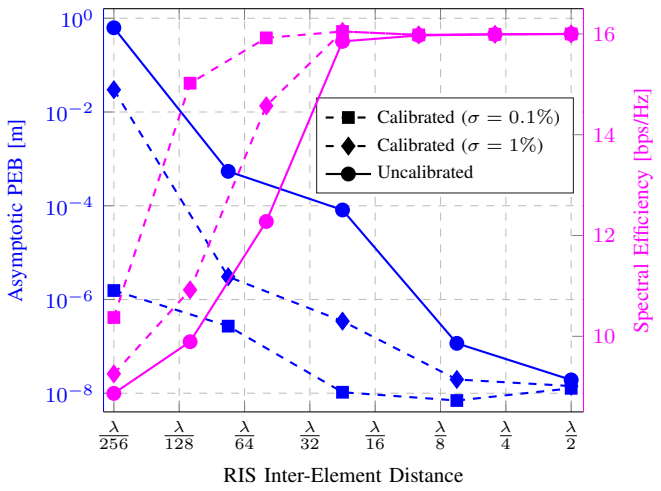

Fig. 4. Asymptotic PEB (localization performance, Fig. 2) and spectral efficiency (communication performance) are analyzed against the RIS inter-element distance in a RIS-aided system with a single-antenna transmitter, a 16-antenna receiver, and a 64-element passive RIS at 30 GHz. Both RIS and receiver arrays use uniform linear arrays. The RIS inter-element distance varies, while the receiver spacing is fixed at half-wavelength. Coupling parameters are computed from Z-parameters [7, Eq. (2)] and converted to S-parameters, where λ is the signal wavelength. Smaller inter-element spacing causes stronger mutual coupling. Calibrated cases assume noisy prior knowledge of S-parameters, with relative residual error σ. Localization uses random beamformers, while communication employs optimal beamforming based on estimated $\hat{S}$ and perfect channel state information via a successive convex approximation optimization algorithm.

provide context, we briefly outline base station (BS) calibration in the positioning system based on the 3rd Generation Partnership Project (3GPP) specification. We also describe joint RIS calibration and user localization systems. Finally, we summarize two calibration methodologies: model-based (described in sections III-A and III-B) and learning-based (given in Sec. III-C) in Table I, along with the deployment of different RIS architectures. As shown, we outline the pros and cons, algorithm complexity, environment adaptability, and specific implementation requirements of each approach, as well as their suitability across different RIS types. While the underlying calibration principles apply broadly, the choice of algorithms and parameters may vary depending on the RIS architecture and associated hardware capabilities. For example, HRIS captures signals from the UE or BS to estimate AOA and TOA, reducing algorithm complexity (see Sec. II-D). However, the split coefficient introduces a new calibration dimension. All discussed calibration methods are applicable to practical scenarios such as indoor localization and vehicular networks. In these dynamic environments, in-situ calibration complements offline methods by enabling real-time adaptation to mobility and environmental changes, helping maintain performance as geometry and hardware impairments evolve.

A. Geometry Calibration

1) Standard Approaches: For BS calibration in uplink (UL) positioning systems, a reference UE with a known location transmits a sounding reference signal (SRS) to the BS. The BS then estimates its own location and compares it with the true location to determine correction terms for other UEs [13, Ch.5.4.5]. For downlink (DL) positioning calibration, the reference UE performs measurements (e.g., TOA and AOA) and reports these to the BS. A similar process is used for UL positioning as for the DL.

2) RIS-aided Systems: In a RIS-aided ISAC system, RIS geometry calibration is required in addition to BS calibration. During this process, it is assumed that hardware impairment parameters are known or can be estimated, implying that hardware and geometry calibration are performed iteratively. Note that the RIS geometry calibration process can be on-demand (e.g., upon installation or after maintenance) or periodic (e.g., for mobile RIS), introducing overhead and delay.

RIS geometry calibration can be performed using multi-static or bi-static sensing systems in UL or DL scenarios under time division duplex (TDD) mode. Certain UE anchors (reference UEs) with known states transmit or receive signals to/from the BS via the RIS. Based on received signals at the BS or reference UEs, measurements are extracted per their capabilities. Anchors with high-bandwidth signaling can measure TOA, while those with antenna arrays capture AOA/AOD. A key challenge in highly correlated channels is resolving individual paths, especially the LoS path between RIS and BS, critical for calibration. Systems with high bandwidth and large antenna arrays can effectively resolve multipath components. These measurements are estimated via maximum-likelihood estimators or advanced techniques like compressed sensing, MUltiple SIgnal Classification (MUSIC), and Estimation of Signal Parameters via Rotational Invariance Technique (ESPRIT). The RIS state is then estimated through triangulation among BS, reference UEs, and RIS using TOA and AOA/AOD. For mobile RIS, Doppler measurements and algorithms like the Kalman filtering may be needed. Errors in TOA, AOA, and Doppler affect RIS position/orientation, requiring proper modeling (e.g., using Bayesian methods). Geometry calibration applies to both NF and FF regimes, with NF calibration being more complex.

The aforementioned approach can be extended to *calibrate the RIS geometry and estimate the UEs locations jointly*. The feasibility of such a system depends on having a sufficient number of measurements relative to the number of unknown states, meaning that the number of geometric observations must exceed the number of geometric unknowns. In this system, known as joint RIS geometry calibration and UE localization [12], the RIS can utilize any of the previously mentioned architectures. However, having sensing capability at the RIS can provide additional measurements, thereby reducing the complexity of the localization algorithm. Moreover, the computational complexity of this method varies depending on the practical application. For instance, indoor localization, where the owner can change the RIS location (e.g., by moving it on a wall), may involve less computational complexity compared to mobile RIS.

B. Hardware Calibration

1) Standard Approaches: For BS calibration in positioning systems, certain hardware calibrations, such as antenna calibration and beam pattern measurements, are performed offline in a factory setting, often within an anechoic chamber. However, online calibration is also necessary due to factors such as

temperature changes during normal operation, which can affect the frequency response of the antenna system and impact BS performance. This can be performed via self-calibration, where pilot signals are transmitted from each antenna to a reference antenna to estimate relative calibration coefficients. Applying these coefficients compensates for phase and amplitude differences among antennas, ensuring reciprocity in TDD systems. Unlike UE-based methods, it requires no UE feedback, and the calibration remains valid longer since BS antennas do not experience clock drift. However, for other calibration scenarios described in our manuscript (e.g., detecting and correcting hardware failures unrelated to temperature changes) regular hardware monitoring is employed. Upon detecting errors, the system rapidly identifies the issue's source and immediately initiates calibration using signals received from the UE, ensuring uninterrupted and optimal hardware performance.

2) RIS-aided Systems: A specific challenge with RIS is *beam calibration*, which is a foundational requirement for ISAC systems, where any error in beam calibration leads to inaccuracies in the RIS AOA or AOD estimates. This type of calibration is similar to antenna array beam calibration, ensuring that beams point correctly while accounting for power responses and grating lobes, which support null direction identification. Beam calibration is performed both in the factory (typically in an anechoic chamber) and at runtime, with the help of reference UEs at known directions relative to the RIS. During this process, the phase difference between two adjacent antennas is removed to prevent additional phase shifts from being introduced into the beamforming vectors. Note that during factory calibration, all predefined beams (e.g., the beam for synchronization signal block (SSB) in the 5G system) are checked to ensure they point in the expected direction.

RIS hardware calibration can be performed offline, similar to BS calibration. For example, RIS calibration to address hardware impairments such as mutual coupling can be conducted offline; however, this process is time-consuming and may become impractical once the RIS is deployed. Moreover, hardware failures (e.g., pixel failures) can occur during operation, necessitating online calibration for ongoing monitoring. Online hardware calibration, which assumes that geometry calibration is available, typically estimates unknown hardware parameters using a signal model. This calibration is performed using an agent-based approach, which is consistent with the geometry-based calibration method described in Sec. III-A.

Agent-based *RIS hardware calibration can be conducted jointly with UE localization*. For instance, in the context of pixel failures, joint localization and failure diagnosis (JLFD) can be performed, where the UE diagnoses RIS pixel failures as part of the hardware calibration while simultaneously estimating its location [10]. Figure 5 illustrates the performance of JLFD along with the theoretical bounds on the localization when $p_{\text{fail}} = 1\%$. The performance is compared to failure-agnostic estimator (which ignores the presence of failures) saturates at high SNRs (attaining the corresponding bound quantified by the LB) since the mismatch between the true model with failures and the ideal model without failures becomes the dominating factor. On the other hand, the JLFD algorithm can largely close the performance gap to the ideal case without failures (quantified by the PEB) by effectively taking into account the presence of failures.

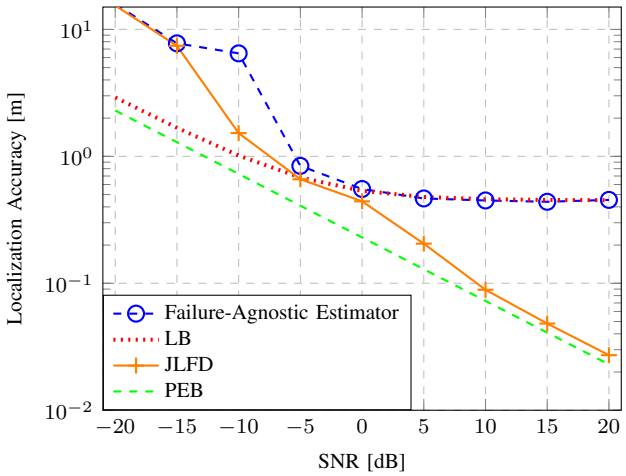

Fig. 5. Localization RMSE vs. SNR obtained by the failure-agnostic estimator and the joint localization and failure diagnosis (JLFD) estimator along with the corresponding theoretical bounds when $p_{\text{fail}} = 1\%$. PEB provides a theoretical limit on localization accuracy when the user has perfect knowledge of pixel failure mask. The same setup as in Fig. 3(a) is considered.

C. Learning-based Calibration

The aforementioned calibration methods are typically used when *accurate and simple* signal and hardware models are available in RIS-aided ISAC systems. However, when an accurate model is not available, is overly complicated, or when dealing with an accurate generative model with unknown parameters, machine learning methods are preferred [14].

1) Fingerprinting: When we lack information about the channel model, we can use black-box deep learning. In fingerprinting-based localization, a supervised machine learning-based approach learns a function mapping the observed signal to the UE location. In this case, the calibration process is implicitly part of the training phase to learn the true model. However, such pure data-driven approaches often require extensive training data to capture the nuances of hardware impairments and environmental conditions, which may not always be available in practical scenarios. A key scalability issue is overfitting, where a model trained too closely to specific conditions may perform poorly under slightly different operational scenarios.

2) Model-driven Deep Learning: When we have an accurate generative model, but with unknown parameters, model-based deep learning can be applied. In [14], the calibration model is integrated into the learning framework. On the one hand, the complexity of calibration models can be reduced through a learning-based surrogate model, which extracts model features and decreases the number of measurement cycles needed for calibration [15]. On the other hand, a sufficient number of measurements is required for classical calibration methods. Additionally, high-dimensional calibration parameters can be included as part of the trainable neural network parameters, which can be conveniently optimized within machine learning frameworks. In this context, operation

TABLE I
SUMMARY OF RIS CALIBRATION METHODOLOGIES AND REMARKS ON DIFFERENT RIS TYPES

Methodology or RIS Architecture		Algorithm Complexity	Environment Adaptability	Pros	Cons	Remark
Model-based	Standard calibration	Medium	Medium	Clear calibration task formulation	High cost with the agent, accurate model needed	Works for both geometry and hardware
	Joint localization and calibration	High	High	Practical onsite calibration	High complexity or extra processing unit needed	Calibration model needed
Learning-based	Fingerprinting	Very high	Low	Calibrates all parameters at once	Large dataset required, less scalable, sensitive to environment change	Learns the signal-to-state mapping
	Model-driven Deep Learning	High	Medium	Small dataset, fast training	Accurate model needed	Learns the calibration parameters
PRIS (low hardware cost)		High	High	Low deployment cost	Challenging channel estimation, weak signal	Processing at the receiver side
HRIS (high hardware cost)		Medium	Medium	Low complexity algorithm, local measurements at RIS	High overhead signaling and high cost implementation	Extra processing capability, power split coefficient calibration
ARIS (high hardware cost)		High	Medium	Enhances received SNR	Introduced colored noise, and additional power consumption	Signal amplification capability, power amplifier calibration
STAR-RIS (high hardware cost)		High	Medium	Capability of indoor and outdoor coverage	Hardware cost, working mode selection	Wide service areas, split coefficient calibration
BD-RIS (very high hardware cost)		Very high	Low	Performance gain over diagonal RIS	More hardware failures, more parameters need to be calibrated due to additional connections	New models and algorithms required

* Calibration frequency depends on the nature of the task and the type of impairment. Low-frequency: Geometry, time-invariant hardware impairments (HWIs) such as mutual coupling, split coefficients; Medium-frequency: moderately time-varying HWIs such as pixel failure, non-ideal beam pattern. High-frequency: highly dynamic HWIs such as phase noise and clock bias. Note that *environment adaptability*, as mentioned above, refers to the capability of a RIS calibration method or RIS architecture to maintain effective performance under varying or dynamic environmental conditions.

over the real, uncalibrated channel is crucial. Supervised learning and reinforcement learning can be applied to receiver learning and transmitter learning, respectively.

The implementation of learning-based calibration in RIS-aided systems is largely similar to BS calibration. However, the online optimization of RIS profiles may introduce extra training complexity. Thus, the appropriate learning framework should be selected, balancing the benefits of improved performance against the costs of implementation and maintenance. Moreover, learning-based calibration is fundamentally an estimation problem, making it susceptible to errors that can degrade positioning performance. These errors can be minimized by incorporating additional UE-BS-RIS measurements during training. While this approach works well for static RIS, mobile RIS calibration is more challenging due to constantly changing conditions, necessitating a diverse and extensive training set. To address this, an artificial database generated from a ray-tracing simulator can be used for offline model training, improving practicality in real-world applications. Additionally, updating the partially trained model using offline synthetic data along with dense pilots received frequently from the UE, while applying learning methods such as transfer learning, could be a promising approach.

IV. CHALLENGES AND FUTURE DIRECTIONS

In this paper, we have demonstrated that RIS calibration is crucial for unlocking ISAC capabilities. Both geometric and hardware calibration are required to avoid severe performance penalties for communication, but especially for localization and sensing. Therefore, we argue that all RIS-based ISAC work should take calibration aspects into account. This paper has only addressed a few selected topics in this area, and many challenges remain unsolved.

1) *Weak signal of the RIS path:* Calibration is conducted based on measurements obtained via the reflected path from the RIS to the BS, which tends to be weak. This presents a significant challenge in RIS calibration. One potential solution is to amplify the reflected path (i.e., using active RIS). However, such a technique comes with its own challenges (as discussed in Sec. II-D). Finally, intentionally blocking the direct path can help tackle this issue, although the direct path is useful for clock bias, especially when joint RIS calibration and UE localization are considered.
2) *Extra large RIS:* Online joint localization and calibration becomes challenging with increasing RIS sizes. Detecting impairments in individual RIS elements relying on few transmissions in a coherent processing interval

requires sophisticated, high-complexity algorithms and realistic modeling of RIS hardware. Future research should focus on low-complexity and data-driven calibration algorithms to circumvent the issues of RIS model deficiency.

3) *Cooperative calibration:* Sidelink communication between UEs can extend communication coverage, which is also helpful for localization and sensing. Additional information between collaborative UEs can reduce the time for calibration. Moreover, cooperative positioning can provide more calibration agents, while multiple positions of the UEs can improve performance (e.g., reduced blind areas and better beam calibration on different angles). Coordination and resource management are the key to realize cooperative calibration.
4) *Computational complexity of the calibration system*: The complexity of RIS calibration depends on various factors, including the RIS topology, RIS size, the number of measurements required for calibration, RIS deployment (i.e., static or mobile), and the practical application, which in some cases demands a high calibration rate due to hardware or positional changes influenced by factors such as temperature or damage. For instance, the calibration process becomes more challenging when employing a large mobile RIS while simultaneously localizing the UE. In addition, the essential communication between the BS and RIS for transferring measurements can also introduce complexity to the system.
5) *Complex environments:* Calibration can be viewed as an estimation problem integrated with sensing tasks. However, in real-world scenarios, the presence of multipath effects introduces additional unknowns, significantly increasing the complexity of calibration. This means that joint calibration and localization tasks must account for multipath in these scenarios. Yet, with a detailed map of the surrounding environment, these multipath effects can be leveraged to aid in calibration. Specifically, a strong reflector with a known state can be used to counteract the impact of that path and even provide geometric information to enhance positioning accuracy.

REFERENCES

[1] J. Hu *et al.*, "Reconfigurable Intelligent Surface based RF Sensing: Design, Optimization, and Implementation," *IEEE J. Sel. Areas Commun.*, vol. 38, no. 11, pp. 2700–2716, 2020.

[2] E. Basar *et al.*, "Wireless Communications Through Reconfigurable Intelligent Surfaces," *IEEE Access*, vol. 7, pp. 116 753–116 773, Aug. 2019.

[3] M. Ahmed *et al.*, "Active Reconfigurable Intelligent Surfaces: Expanding the Frontiers of Wireless Communication-A Survey," *IEEE Commun. Surveys Tuts.*, pp. 1–1, 2024, early access.

[4] S. Mano and T. Katagi, "A Method for Measuring Amplitude and Phase of Each Radiating Element of a Phased Array Antenna," *Electron. Commun. Japan (Part I: Commun.)*, vol. 65, no. 5, pp. 58–64, 1982.

[5] J. Zhao *et al.*, "Localization of Wireless Sensor Networks in the Wild: Pursuit of Ranging Quality," *IEEE/ACM Trans. Netw.*, vol. 21, no. 1, pp. 311–323, 2012.

[6] H. Taghvaee *et al.*, "Error Analysis of Programmable Metasurfaces for Beam Steering," *IEEE J. Emerg. Sel. Topics Circuits Syst.*, vol. 10, no. 1, pp. 62–74, 2020.

[7] P. Zheng, X. Ma, and T. Y. Al-Naffouri, "On the Impact of Mutual Coupling on RIS-Assisted Channel Estimation," *IEEE Wireless Commun. Lett.*, vol. 13, no. 5, pp. 1275–1279, 2024.

[8] S. Abeywickrama *et al.*, "Intelligent Reflecting Surface: Practical Phase Shift Model and Beamforming Optimization," *IEEE Trans. Commun.*, vol. 68, no. 9, pp. 5849–5863, 2020.

[9] S. Fortunati *et al.*, "Performance Bounds for Parameter Estimation Under Misspecified Models: Fundamental Findings and Applications," *IEEE Signal Process. Mag.*, vol. 34, no. 6, pp. 142–157, 2017.

[10] C. Ozturk *et al.*, "Ris-Aided Localization Under Pixel Failures," *IEEE Trans. Wireless Commun.*, 2024.

[11] R. Ghazalian *et al.*, "Joint User Localization and Location Calibration of a Hybrid Reconfigurable Intelligent Surface," *IEEE Trans. Veh. Technol.*, 2023.

[12] P. Zheng *et al.*, "JrCUP: Joint RIS calibration and User Positioning for 6G Wireless Systems," *IEEE Trans. Wireless Commun.*, 2023.

[13] 3GPP, "NG Radio Access Network (NG-RAN); Stage 2 Functional Specification of User equipment (UE) positioning in NG-RAN. Release 16," 3rd Generation Partnership Project, Tech. Rep. GPP TS 38.305 V18.2.0, Jun. 2024, release 18.

[14] Y. Ma *et al.*, "Learn to Communicate With Neural Calibration: Scalability and Generalization," *IEEE Trans. Wireless Commun.*, vol. 21, no. 11, pp. 9947–9961, 2022.

[15] Z. Zhou *et al.*, "Transfer-Learning-Assisted Multielement Calibration for Active Phased Antenna Arrays," *IEEE Trans. Antennas Propag.*, vol. 71, no. 2, pp. 1982–1987, 2022.

Reza Ghazalian (reza.ghazalian@nokia.com; ext-reza.ghazalian@aalto.fi) is a senior RF Specification Engineer at Nokia Mobile Network, and a visiting researcher at Aalto University, Espoo, Finland. His research interests include RIS, radio localization, signal processing and optimization.

Pinjun Zheng (pinjun.zheng@kaust.edu.sa) is a PhD candidate at KAUST, Saudi Arabia. His research interests include signal processing for 5G/6G localization and communication applications.

Hui Chen (hui.chen@chalmers.se) is a postdoctoral researcher at Chalmers University of Technology, 41296 Gothenburg, Sweden. His research interests include mmWave/THz and RIS-aided localization.

Cuneyd Ozturk (cuneyd93@gmail.com) is a lead engineer at Aselsan Inc., Ankara, Turkey. His research interests include satellite communication networks and RIS-aided localization.

Musa Furkan Keskin (furkan@chalmers.se) is a research specialist at Chalmers University of Technology, Gothenburg, Sweden. His current research interests include integrated sensing and communications, RIS-aided localization and sensing, and hardware impairments in beyond 5G/6G systems.

Vincenzo Sciancalepore (vincenzo.sciancalepore@neclab.eu) is a Principal Researcher at NEC Laboratories Europe, Germany, focusing his activity on RISs. He is an editor of IEEE Transactions on Wireless Communications and IEEE Transactions on Communications.

Sinan Gezici (gezici@ee.bilkent.edu.tr) is a professor at Bilkent University, Ankara, Turkey. His research interests include statistical signal processing, visible light systems, and wireless localization.

Tareq Y. Al-Naffouri (tareq.alnaffouri@kaust.edu.sa) is a professor at KAUST, Saudi Arabia. His research interests include sparse, adaptive, and statistical inference/learning and their applications to wireless communications, localization, smart cities, and smart health.

Henk Wymeersch (henkw@chalmers.se) is a professor at Chalmers University of Technology, 41296 Gothenburg, Sweden. His research interests include 5G and beyond 5G radio localization and sensing.